

Collective properties of the odd-mass Cs nuclei. II.  $^{119,121,123,125}\text{Cs}$ U. Garg,\* T. P. Sjoreen,<sup>†</sup> and D. B. Fossan

Department of Physics, State University of New York, Stony Brook, New York 11794

(Received 2 August 1978)

Using the techniques of in-beam  $\gamma$ -ray spectroscopy, the high-spin states in the odd-mass  $^{119-125}\text{Cs}$  have been studied via the  $^{106}\text{Cd}(^{16}\text{O}, p2n)^{119}\text{Cs}$ ,  $^{110-114}\text{Cd}(^{14}\text{N}, 3n)^{121-125}\text{Cs}$ , and  $^{116,118}\text{Sn}(^{10}\text{B}, 3n)^{123,125}\text{Cs}$  reactions on enriched, self-supporting targets. Two distinct collective features are observed in the resulting level schemes:  $\Delta J = 2$  bands built on the  $11/2^-$  ( $1h_{11/2}$  quasi-proton) states, and  $\Delta J = 1$  bands built on the  $9/2^+$  ( $1g_{9/2}$  proton-hole) states. The  $9/2^+$  bandheads, believed to result from the excitation of the  $1g_{9/2}$  proton across the  $Z = 50$  closed shell, are observed at surprisingly low energies, becoming the ground state in  $^{119}\text{Cs}$ . The systematics of the  $9/2^+$   $\Delta J = 1$  bands are presented and discussed in terms of the particle-plus-rotor and particle-plus-vibrator models. A deformed structure relationship between the excitation of a  $1g_{9/2}$  proton and the excitation of a pair of  $1g_{9/2}$  protons across the  $Z = 50$  closed shell is discussed.

NUCLEAR REACTIONS  $^{106}\text{Cd}(^{16}\text{O}, p2n)^{119}\text{Cs}$ ,  $^{110-114}\text{Cd}(^{14}\text{N}, 3n)^{121-125}\text{Cs}$ ,  $^{116,118}\text{Sn}(^{10}\text{B}, 3n)^{123,125}\text{Cs}$ ; measured  $\gamma$ - $\gamma$  coincidence,  $\gamma(E, \theta)$ ; deduced level schemes in odd-mass  $^{119-125}\text{Cs}$ ,  $\gamma$  multiplicities,  $J^\pi$ . Enriched targets, Ge (Li) detectors.  
NUCLEAR STRUCTURE Odd-mass  $^{119-125}\text{Cs}$ , calculated  $\frac{9}{2}^+$   $\Delta J = 1$  rotational bands.

## I. INTRODUCTION

The recent availability of rich high-spin spectra for odd-mass nuclei near the  $Z = 50$  closed shell has aided considerably in the understanding of the nature of the collectivity in this transitional region. A very interesting feature of the odd-mass nuclei above the  $Z = 50$  closed shell has been the observation of  $\Delta J = 1$  rotational bands built on low-lying deformed  $\frac{9}{2}^+$  proton-hole states in odd-mass Sb ( $Z = 51$ ) and I ( $Z = 53$ ) nuclei. To further map out the behavior of these states, which seem to have a large deformation, and to understand their coexistence with states of more modest deformations, an experimental investigation of the collective states in odd-mass Cs ( $Z = 55$ ) nuclei has been carried out over the mass range  $A = 119-133$ . In the preceding paper,<sup>1</sup> hereinafter referred to as paper I, the results for  $^{127,129,131,133}\text{Cs}$  were presented and the systematics of the  $\Delta J = 2$  bands built on  $\frac{5}{2}^+$ ,  $\frac{7}{2}^+$ , and  $\frac{11}{2}^+$  levels were discussed. This paper presents the detailed results on  $^{119,121,123,125}\text{Cs}$ .

In addition to the  $\Delta J = 2$  bands built on the  $\frac{7}{2}^+$  and  $\frac{11}{2}^+$  levels, which have been discussed in detail in paper I, a series of  $\Delta J = 1$  bands built on low-lying  $\frac{9}{2}^+$  states have been observed in the odd-mass  $^{119-125}\text{Cs}$  nuclei. The  $\frac{9}{2}^+$  bandheads are believed to result from the excitation of a  $1g_{9/2}$  proton across the  $Z = 50$  closed shell and have been observed previously in odd-mass Sb and I nuclei. This structure has been implied for the Sb isotopes by  $L = 4$  Te( $t, \alpha$ ) pickup<sup>2</sup> and by  $L = 0$  In( $^3\text{He}, n$ ) transfer.<sup>3</sup> The  $\frac{9}{2}^+$  bandheads are ob-

served at surprisingly low excitation energies, becoming the ground state in  $^{119}\text{Cs}$ ; this drop in energy has been attributed to the deformation of the core.<sup>4,5</sup> A deformed-structure relationship between the excitation of the  $1g_{9/2}$  proton and the excitation of a pair of  $1g_{9/2}$  protons across the  $Z = 50$  closed shell has recently been made.<sup>6,7</sup> These features will be discussed in detail in Sec. IV. A brief report on these  $\Delta J = 1$  bands was made in an earlier publication<sup>6</sup>; several preliminary reports have also been made.<sup>8</sup>

## II. EXPERIMENTAL PROCEDURE

The reactions used for populating the odd-mass Cs nuclei in this study, are summarized in Table I. The heavy-ion beams were provided by the Stony Brook FN tandem Van de Graaff accelerator. The following in-beam measurements were performed, using Ge(Li) detectors: excitation functions,  $\gamma$ - $\gamma$  coincidence and  $\gamma$ -angular distributions. The details of the experimental procedures have been described in paper I.<sup>1</sup>

## III. EXPERIMENTAL RESULTS

The results of the  $\gamma$ - $\gamma$  coincidence measurements are summarized in Tables II-V, respectively, for  $^{119}\text{Cs}$ ,  $^{121}\text{Cs}$ ,  $^{123}\text{Cs}$ , and  $^{125}\text{Cs}$ . In Tables VI and VII, the results of the angular distribution measurements for  $^{123}\text{Cs}$  and  $^{125}\text{Cs}$  are summarized. Primarily because of the considerable photopeak doppler shifts at back angles, precise  $A_2$  and  $A_4$  coefficients could not be extracted from the angular distribution results for  $^{119}\text{Cs}$  and  $^{121}\text{Cs}$ .

TABLE I. Reaction information for  $^{119-125}\text{Cs}$ .

Nucleus	Reaction used	Target thickness mg/cm <sup>2</sup>	Beam energy <sup>a</sup> MeV
$^{119}\text{Cs}$	$^{106}\text{Cd}[^{16}\text{O}, p2n]^{119}\text{Cs}$	3.5	72
$^{121}\text{Cs}$	$^{110}\text{Cd}[^{14}\text{N}, 3n]^{121}\text{Cs}$	2.3	58
$^{123}\text{Cs}$	$^{116}\text{Sn}[^{10}\text{B}, 3n]^{123}\text{Cs}$	10.0	44
	$^{112}\text{Cd}[^{14}\text{N}, 3n]^{123}\text{Cs}$ <sup>b</sup>	3.0	58
$^{125}\text{Cs}$	$^{118}\text{Sn}[^{10}\text{B}, 3n]^{125}\text{Cs}$	10.1	41
	$^{114}\text{Cd}[^{14}\text{N}, 3n]^{125}\text{Cs}$ <sup>b</sup>	10.0	56

<sup>a</sup> Energy used for  $\gamma$ - $\gamma$  and  $W(\theta)$  measurements.

<sup>b</sup> Only singles measurements performed for this reaction.

Two features are common to all these nuclei. The first is  $\Delta J=2$  cascades built on the low-lying  $\frac{11}{2}^-$  levels. The spacings in these cascades are very similar to the ground-state band spacings in the corresponding  $(^{A-1})\text{Xe}$  core nuclei. The angular distributions of the cascade members yielded  $A_2$  and  $A_4$  coefficients characteristic of pure  $J \rightarrow J-2$  quadrupole transitions. Similar  $\Delta J=2$  cascades built on  $\frac{11}{2}^-$  levels have been observed in the higher odd-mass Cs nuclei. In all the Cs isotopes reported in this paper, the  $\frac{11}{2}^-$  level appears to be a long lived isomer. Since no other  $\gamma$  rays are observed in coincidence with these cascades, rigorous spin assignments for all of the  $\frac{11}{2}^-$  bandheads are not possible and, in those cases, have been assumed on the basis of the systematics of this feature in the odd-mass Cs as well as other odd-proton nuclei in this region. These assignments are consistent with the lifetimes of these isomers, where known, and in some cases, are further supported by the angular distributions of  $\gamma$  rays connecting the  $\frac{11}{2}^-$  level with other levels in those nuclei.

The second feature common to these nuclei is a

TABLE II.  $\gamma$ - $\gamma$  coincidence results for  $^{119}\text{Cs}$ .

$E_\gamma$ (keV)	$\gamma$ rays in coincidence <sup>a</sup>
240	269, 297, 322, (344), (566), (619), (667)
269	240, 297, 322, (344), (619)
288	475, 618, 734
297	240, 269, 322
322	240, (269), (344)
344	(240), (269), (297)
475 <sup>b</sup>	288, 618, 734.
618	288, 475, 734
619	(240), (269)
734	288, 475, 618

<sup>a</sup> Parentheses denote weak coincidences.

<sup>b</sup> Doublet.

TABLE III.  $\gamma$ - $\gamma$  coincidence results for  $^{121}\text{Cs}$ .

$E_\gamma$ (keV)	$\gamma$ rays in coincidence <sup>a</sup>
246	171, <sup>b</sup> 276, 304, 328, 347, 361, 367, 580, 632, 675, 708, 728
276	245, 304, 328, 347, 361, 367, 632, 675, 708
286	472, 615, 726, (779), 816
304	246, 276, 328, 347, 361, 367, 522, 675, 728
328	184, <sup>b</sup> 246, 276, 304, 347, (361), 367, 522, 580, (708)
347	246, 276, 304, 328, 361, 367, 522, 580, (632), 728
361	246, 276, 304, 328, 347, 367, (522), 675
367	246, 276, 304, 328, 347, 361, (708)
472 <sup>c</sup>	186, <sup>b</sup> 286, 615, 726, 816
522	304, 328, (632)
580	246, 328
615 <sup>c</sup>	286, 472, 726, 816
632	246, 276, (347), (361)
675	246, 276, 304, 361, 580
708	246, 276, (304), (328), (632)
726	286, 472, 615, 816
728	246, 276, 304, (328), (580), (632), (675)
816	286, 472, 615, 726

<sup>a</sup> Parentheses denote weak coincidences.

<sup>b</sup> Not included in the level scheme.

<sup>c</sup> Doublet.

TABLE IV.  $\gamma$ - $\gamma$  coincidence results for  $^{123}\text{Cs}$ .

$E_\gamma$ (keV)	$\gamma$ rays in coincidence <sup>a</sup>
64	95
95 <sup>b</sup>	54, <sup>c</sup> (64), 83, <sup>c</sup> 138, <sup>c</sup> 201, 269, (303)
137	95, 269, 303, (337), (367), 428, (572), (640)
201	95, 269, 303, 337, 367, 428, 599
269	95, 137, 201, (234), <sup>c</sup> 303, 337, 367, 389, 640, (705)
303	95, 127, 201, 269, 337, 367, (389), (640), 705
321	(434), 522, 683, 685, 730, 800
337	95, (137), 174, <sup>c</sup> 201, 269, 303, 367, 389, 572, (757)
367	(201), 269, 303, 337, (389), (572), (640)
428	137, 201, 599
434	321, 683
522	321, 685, 730, 800
572	(95), 201, (705)
599 <sup>b</sup>	201, 428, 560, <sup>c</sup> 615 <sup>c</sup>
640	201, 269, (303), (560) <sup>c</sup>
683	321, 434, 701
685	321, 522, 800
701	(321), (434), 683
705	(95), (201), 269, 303
730	321, 522
800	321, 522, 685

<sup>a</sup> Parentheses denote weak coincidences.

<sup>b</sup> Doublet.

<sup>c</sup> Not included in the level scheme.

TABLE V.  $\gamma$ - $\gamma$  coincidence results for  $^{125}\text{Cs}$ .

$E_\gamma$ (keV)	$\gamma$ rays in coincidence <sup>a</sup>
77	176, 189, (365), 430, (610), (647)
85	168, (211), <sup>b</sup> (365), 430
122	181, 246, 312, 365, 647
168	85, 150, <sup>b</sup> (211), <sup>b</sup> 430, 610, 762
176	77, 334, <sup>b</sup> 430, 610, 762
181	122, 246, 312, 365, 647
189 <sup>c</sup>	(77), (365), (572), (647), (760).
246	122, 181, 312, 365, 647
274	309, 346, 377, (655), (723)
309	274, 346, 377, (723)
312	122, 181, (197), <sup>b</sup> 246, 365, 647
346	274, 309, 377
365	122, 181, 246, 312, 475, 572, 647, 671, 696, 760, 870
377	274, 309, 346, (655)
430	77, 85, 168, 176, 610, 762
475	365, 647
572	365, 696, 760, 870
610	(77), (85), 168, 176, 430, 762
647	122, 181, (189), 246, (312), 365, 475, 671, 785
655	(274), (377)
671	365, (475), (647)
696	365, 572
760	365, 572, (870)
762	430, 610
785	(365), (647)
870	365, 572, 760

<sup>a</sup> Parentheses denote weak coincidences.<sup>b</sup> Not included in the level scheme.<sup>c</sup> Doublet.TABLE VI. Angular distribution results for  $^{123}\text{Cs}$ .

$E_\gamma$ <sup>a</sup> (keV)	$I_\gamma$ <sup>b</sup> relative	$A_2$ <sup>c</sup>	$A_4$ <sup>c</sup>	Assignment
94.7				$\frac{5}{2}^+ \rightarrow \frac{1}{2}^+$
136.9	10	$-0.30 \pm 0.05$		$\frac{3}{2}^+ \rightarrow \frac{11}{2}^-$
201.2	16	$0.30 \pm 0.15$	$0.03 \pm 0.18$	$\frac{3}{2}^+ \rightarrow \frac{5}{2}^+$
269.0	21	$0.13 \pm 0.04$	$0.02 \pm 0.05$	$\frac{11}{2}^+ \rightarrow \frac{3}{2}^+$ <sup>d</sup>
303.3	16	$0.08 \pm 0.05$	$-0.08 \pm 0.07$	$\frac{13}{2}^+ \rightarrow \frac{11}{2}^+$ <sup>d</sup>
320.6	100	$0.34 \pm 0.08$	$-0.04 \pm 0.10$	$\frac{15}{2}^- \rightarrow \frac{11}{2}^-$
337.0	12	$0.03 \pm 0.04$	$-0.02 \pm 0.06$	$\frac{15}{2}^+ \rightarrow \frac{13}{2}^+$ <sup>d</sup>
367.4	5			$\frac{17}{2}^+ \rightarrow \frac{15}{2}^+$
388.6	4			$\frac{19}{2}^+ \rightarrow \frac{17}{2}^+$
428.0	10	$0.30 \pm 0.06$	$0.01 \pm 0.08$	$(\frac{13}{2}^+) \rightarrow \frac{9}{2}^+$
434.0	6			$(\frac{13}{2}^-) \rightarrow (\frac{17}{2}^-)$
522.2	69	$0.35 \pm 0.04$	$-0.08 \pm 0.05$	$\frac{13}{2}^- \rightarrow \frac{15}{2}^-$
572.8	9			$\frac{13}{2}^+ \rightarrow \frac{9}{2}^+$
640.3	9	$0.15 \pm 0.09$		$\frac{15}{2}^+ \rightarrow \frac{11}{2}^+$
682.5	20	$-0.29 \pm 0.06$	$-0.02 \pm 0.08$	$(\frac{17}{2}^-) \rightarrow \frac{15}{2}^-$
685.2	36	$0.30 \pm 0.04$	$-0.03 \pm 0.05$	$\frac{23}{2}^- \rightarrow \frac{19}{2}^-$
730.2	15	$-0.60 \pm 0.05$	$0.17 \pm 0.09$	$\frac{21}{2}^- \rightarrow \frac{19}{2}^-$
800.0	14	$0.23 \pm 0.05$	$-0.09 \pm 0.07$	$\frac{27}{2}^- \rightarrow \frac{23}{2}^-$

<sup>a</sup> Energies are within 0.3 keV.<sup>b</sup> Intensities have been normalized to the 320.6 keV line.<sup>c</sup> Wherever not quoted, the values were consistent with 0.0 or were difficult to extract from data because of either a very low peak-to-background ratio or presence of a doublet.<sup>d</sup>  $M1$ - $E2$  transitions with positive mixing ratios (see text).TABLE VII. Angular distribution results for  $^{125}\text{Cs}$ .

$E_\gamma$ <sup>a</sup> (keV)	$I_\gamma$ <sup>b</sup> relative	$A_2$ <sup>c</sup>	$A_4$ <sup>c</sup>	Assignment	$E_\gamma$ <sup>a</sup> (keV)	$I_\gamma$ <sup>b</sup> relative	$A_2$ <sup>c</sup>	$A_4$ <sup>c</sup>	Assignment
77.1	>100			$\frac{5}{2}^+ \rightarrow \frac{1}{2}^+$	474.8	15	$-0.48 \pm 0.08$	$0.27 \pm 0.09$	$(\frac{13}{2}^-) \rightarrow (\frac{17}{2}^-)$
84.6	>140			$\frac{5}{2}^+ \rightarrow \frac{1}{2}^+$	572.0	103	$0.34 \pm 0.07$	$0.07 \pm 0.08$	$\frac{19}{2}^- \rightarrow \frac{15}{2}^-$
121.7	10	$-0.30 \pm 0.06$		$(\frac{23}{2}^-) \rightarrow (\frac{21}{2}^-)$	610.2	19	$0.25 \pm 0.07$	$0.11 \pm 0.09$	$\frac{15}{2}^+ \rightarrow \frac{11}{2}^+$
168.2	136			$\frac{7}{2}^+ \rightarrow (\frac{5}{2}^+)$	647.1	57	$-0.62 \pm 0.05$	$0.05 \pm 0.07$	$(\frac{17}{2}^-) \rightarrow \frac{15}{2}^-$
176.0	100			$\frac{7}{2}^+ \rightarrow \frac{5}{2}^+$	670.9	9	$0.17 \pm 0.11$		$(\frac{23}{2}^-) \rightarrow (\frac{19}{2}^-)$
180.6	11	$-0.46 \pm 0.08$		$(\frac{21}{2}^-) \rightarrow (\frac{19}{2}^-)$	695.5	24	$-0.53 \pm 0.10$	$0.13 \pm 0.13$	$\frac{21}{2}^- \rightarrow \frac{19}{2}^-$
246.4	10	$-0.34 \pm 0.04$		$(\frac{25}{2}^-) \rightarrow (\frac{23}{2}^-)$	759.5	38	$0.29 \pm 0.05$	$-0.06 \pm 0.07$	$\frac{23}{2}^- \rightarrow \frac{19}{2}^-$
311.6	13	$-0.44 \pm 0.05$		$(\frac{19}{2}^-) \rightarrow (\frac{17}{2}^-)$	761.7	10	$0.26 \pm 0.10$	$-0.08 \pm 0.13$	$\frac{19}{2}^+ \rightarrow \frac{15}{2}^+$
365.0	191	$0.31 \pm 0.06$	$0.01 \pm 0.05$	$\frac{15}{2}^- \rightarrow \frac{11}{2}^-$	784.5	5			$(\frac{25}{2}^-) \rightarrow (\frac{23}{2}^-)$
430.0	32	$0.24 \pm 0.04$	$0.04 \pm 0.06$	$\frac{11}{2}^+ \rightarrow \frac{7}{2}^+$	869.5	15	$0.21 \pm 0.07$	$-0.06 \pm 0.10$	$\frac{27}{2}^- \rightarrow \frac{23}{2}^-$

<sup>a</sup> Energies are within 0.3 keV.<sup>b</sup> Intensities have been normalized to the 176.0 keV line.<sup>c</sup> Wherever not quoted, the values were consistent with 0.0 or were difficult to extract from data because of either a very low peak-to-background ratio or presence of a doublet.

series of  $\Delta J=1$  cascades built on low-lying  $\frac{9}{2}^+$  levels. The angular distributions of the  $\gamma$  rays belonging to these cascades exhibit a mixed  $M1-E2$  character with a positive mixing ratio  $\delta$ , i.e., the  $A_2$  coefficients have values close to zero, because the contribution from a positive  $\delta$  largely cancels the dipole contribution. This  $M1-E2$  character of the cascade members is further corroborated by the observation of  $J \rightarrow J-2$   $E2$  crossover transitions.

In several cases, precise angular distribution coefficients could not be obtained because of either very small peak-to-background ratios or considerable photopeak Doppler shifts at back angles. In such cases, the positive or negative nature of the  $A_2$  coefficients has been extracted from a comparison between the  $\gamma$ -ray intensities [ $I_{90^\circ}/I_{150^\circ}$ ] at  $90^\circ$  and  $150^\circ$  angles, respectively. This partial angular distribution information provides definite distinction between dipole and quadrupole transitions.

The individual level schemes of  $^{119,121,123,125}\text{Cs}$  are discussed in detail below.

#### $^{125}\text{Cs}$

Typical  $\gamma$ - $\gamma$  spectra for  $^{125}\text{Cs}$  are shown in Fig. 1 and the resulting level scheme is presented in Fig. 2. The  $\Delta J=2$  cascade, built on the 266-keV  $\frac{11}{2}^-$  level consists of 365-, 572-, 760-, and 870-keV  $\gamma$  rays; and the  $\Delta J=1$  cascade built on the 540-keV  $\frac{9}{2}^+$  level consists of 309-, 346-, and 377-keV  $\gamma$  rays. In addition, another  $\Delta J=2$  cascade built on the 253-keV  $\frac{7}{2}^+$  level has been observed and

consists of 430-, 610-, and 762-keV  $\gamma$  rays. The  $\frac{1}{2}^+$  ground state and the 85-keV  $\frac{5}{2}^+$  level are known from previous work.<sup>9</sup>

The available partial angular distribution information for the members of the  $\Delta J=1$  cascade indicates a mixed  $M1-E2$  character. This is further corroborated by the existence of cross-over transitions of 655 and 723 keV. These  $\gamma$  rays are in coincidence with a 274-keV  $\gamma$  ray which yields an  $I_{90^\circ}/I_{150^\circ}$  value appropriate for a  $J \rightarrow J \pm 1$   $E1$  transition. Since no other  $\gamma$  rays have been observed in coincidence with this cascade, the 274-keV  $\gamma$  ray most probably feeds the  $\frac{11}{2}^-$  isomer at 266 keV.

The isomeric nature of the 266-keV  $\frac{11}{2}^-$  level is suggested by the very weak coincidences observed between the  $\gamma$  rays feeding and depopulating this level. The near isotropic nature of the 85-, 168-, and 176-keV  $\gamma$  rays would, then, result from a substantial delayed cascade feeding from this isomer, via an unobserved 13-keV transition to the 253-keV level, which allows a deterioration of the nuclear alignment by the hyperfine interactions.

The 253-keV level is assumed to be  $\frac{7}{2}^+$  on the basis of the associated  $\Delta J=2$  band structure and its nonisomeric nature; similar  $\Delta J=2$  bands built on the  $\frac{7}{2}^+$  states have been observed in the higher odd-mass Cs isotopes.<sup>1</sup> A small negative  $A_2$  for the 168-keV (prompt)  $\gamma$  ray decaying to the  $\frac{3}{2}^+$  level supports this assumption.

The  $\frac{19}{2}^-$  level at 1203-keV is fed by a  $\gamma$  ray of 696 keV, whose angular distribution exhibits a mixed  $M1-E2$  character ( $\delta \sim -0.23$ ). Hence, the level at 1899 keV has been assigned  $J^\pi = \frac{21}{2}^-$ . The

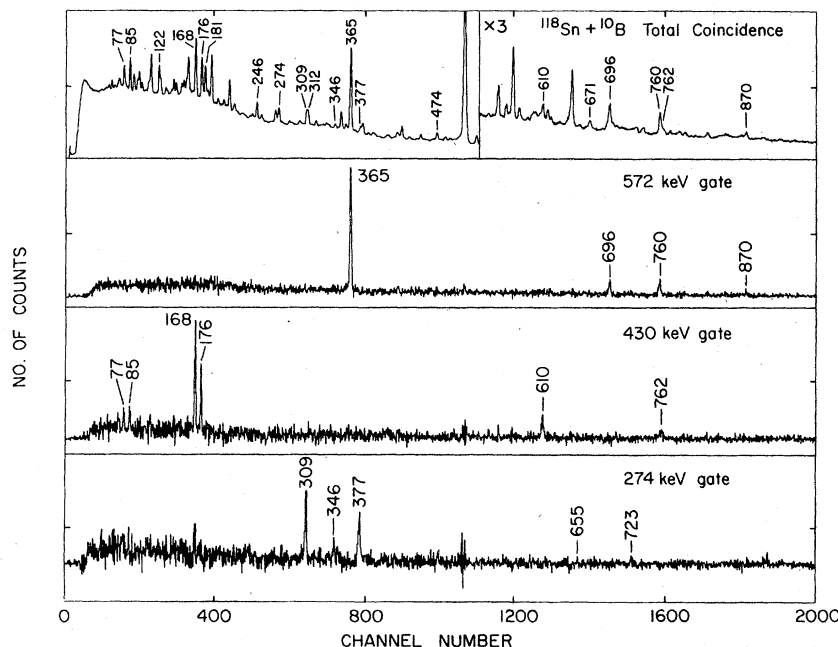


FIG. 1. Typical  $\gamma$ - $\gamma$  spectra for  $^{125}\text{Cs}$ .

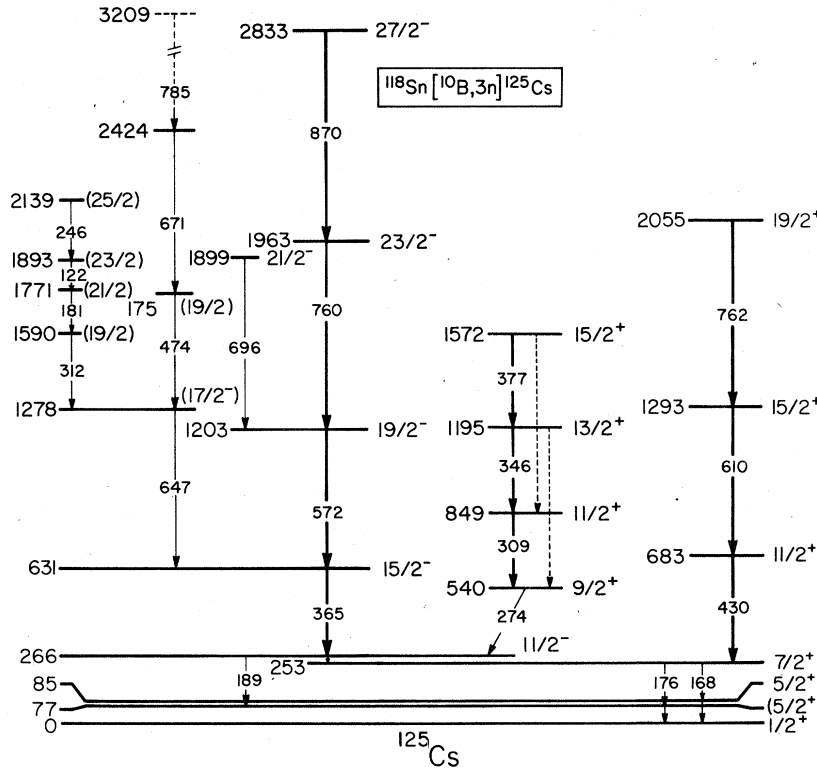


FIG. 2. Level scheme for  $^{125}\text{Cs}$  extracted from the present work. All energies are in keV.

$^{15/2-}$  level at 631 keV is being fed by another strong  $M1-E2$   $\gamma$  ray of 647 keV ( $\delta \sim -0.3$ ), which results in a  $(^{17/2-})$  level at 1278 keV. Two weak cascades of 475-, 671-, 785-keV and 312-, 181-, 122-, 246-keV  $\gamma$  rays are observed on this level. The spin assignments for all the corresponding levels are

tentative.

$^{123}\text{Cs}$

Typical  $\gamma$ - $\gamma$  spectra for  $^{123}\text{Cs}$  are shown in Fig. 3 and the resulting level scheme is presented in Fig. 4. The  $\Delta J=2$  cascade built on the 159-keV

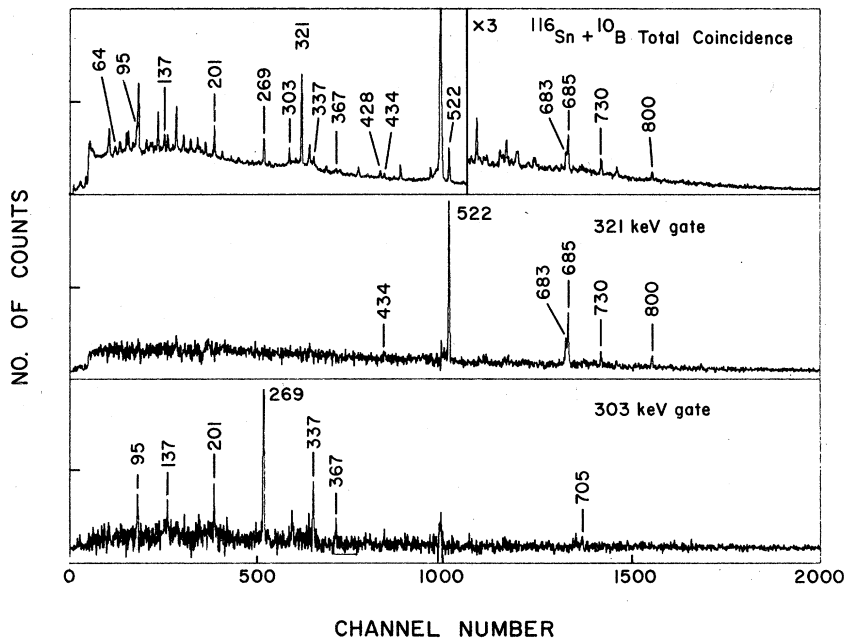


FIG. 3. Typical  $\gamma$ - $\gamma$  spectra for  $^{123}\text{Cs}$ .

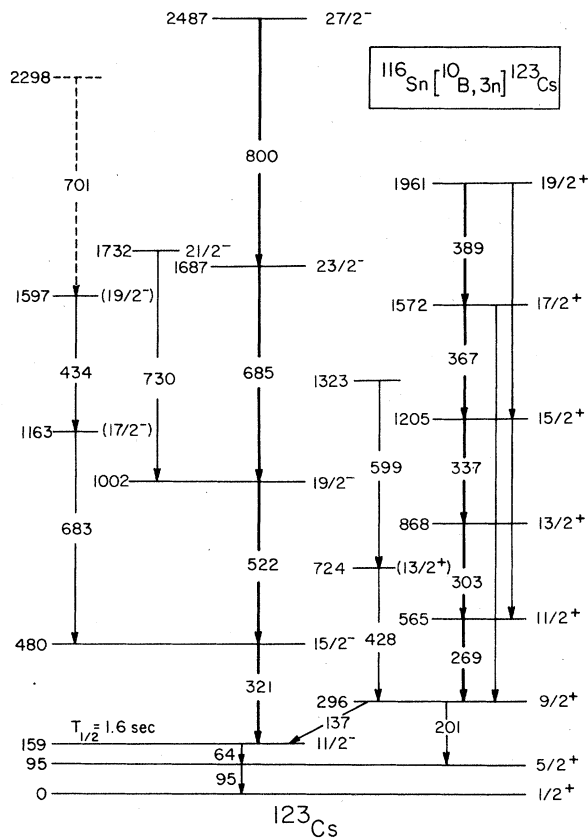


FIG. 4. Level scheme for  $^{123}\text{Cs}$  extracted from the present work. All energies are in keV.

$\frac{11}{2}^-$  isomer consists of 321-, 522-, 685-, and 800-keV  $\gamma$  rays and the  $\Delta J=1$  cascade built on the 296-keV  $\frac{9}{2}^+$  level is made of the 269-, 303-, 337-, 367-, and 389-keV  $\gamma$  rays. The values of  $\delta$  obtained for the 269-, 303-, and 337-keV transitions, using the tables of Der Mateosian and Sunyar,<sup>10</sup> are  $\delta \sim +0.2$ .

The  $\frac{9}{2}^+$  assignment for the 296-keV level is based on the  $J \rightarrow J-2$  quadrupole character of the 201-keV  $\gamma$  ray decaying from this level to the known  $\frac{5}{2}^+$  level at 95 keV.<sup>11</sup> It is consistent with similar states and the associated band structures in other odd-mass Cs as well as Sb and I nuclei. The 137-keV dipole transition from the  $\frac{9}{2}^+$  level supports the  $\frac{11}{2}^-$  spin assumption for the 159-keV level, which is known to be an isomer with  $T_{1/2} = 1.6$  s. This lifetime is consistent with the Weisskopf estimate for a 64-keV  $E3$  transition. A tentative spin assignment of  $(\frac{11}{2}^-)$  for this isomer was suggested by Arlt *et al.*<sup>9</sup>

The  $\frac{19}{2}^-$  level at 1002 keV is fed by a 730-keV  $\gamma$  ray of mixed  $M1-E2$  character ( $\delta \sim -0.27$ ), giving a  $\frac{21}{2}^-$  assignment for the 1732-keV level. The  $\frac{15}{2}^-$  level at 480 keV is fed by a cascade of 683-, 434-, 701-keV  $\gamma$  rays and the 296-keV  $\frac{9}{2}^+$  level is also fed by two cascading  $\gamma$  rays of 428 and 599 keV; the spin assignments for the corresponding levels are tentative.

$^{121}\text{Cs}$

Typical  $\gamma$ - $\gamma$  spectra for  $^{121}\text{Cs}$  are shown in Fig. 5 and the resulting level scheme is presented in Fig. 6. The two distinct features of this nucleus are a  $\Delta J=1$  cascade, consisting of 246-, 276-,

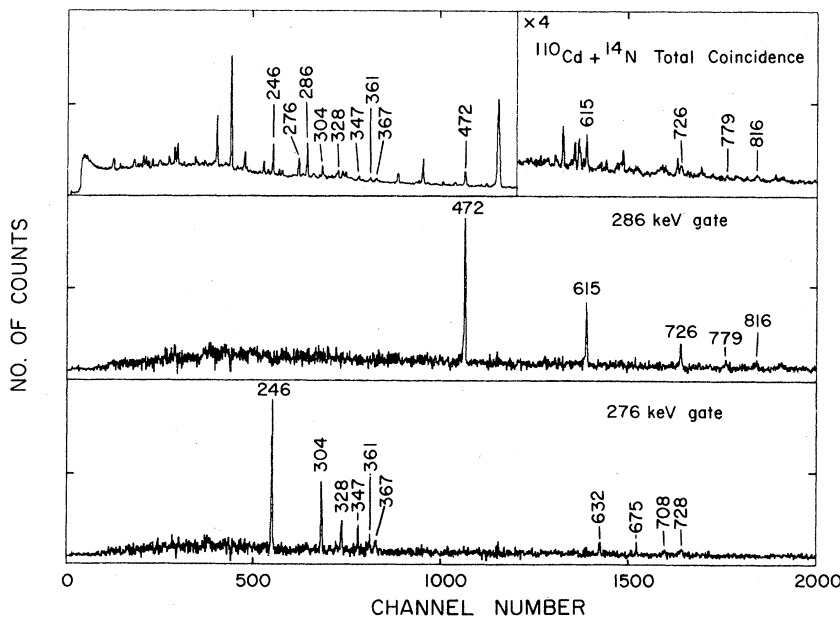


FIG. 5. Typical  $\gamma$ - $\gamma$  spectra for  $^{121}\text{Cs}$ .

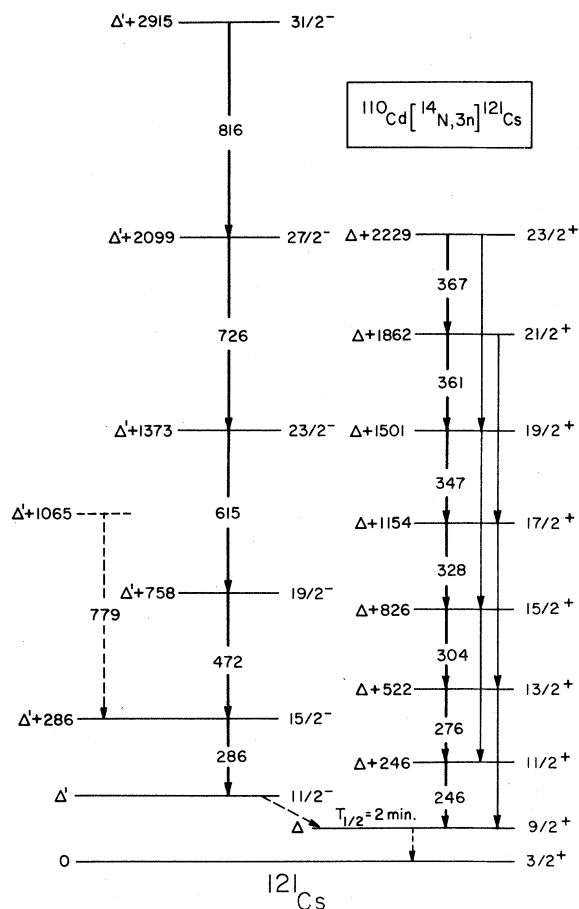


FIG. 6. Level scheme for  $^{121}\text{Cs}$  extracted from the present work. All energies are in keV. The energy  $\Delta$  of the  $\frac{9}{2}^+$  level and  $\Delta'$  of the  $\frac{11}{2}^-$  level are not known (see text).

304-, 328-, 347-, 361-, and 367-keV  $\gamma$  rays built on the  $\frac{9}{2}^+$  level, and a  $\Delta J=2$  cascade, of 286-, 472-, 615-, 726-, and 816-keV  $\gamma$  rays built on the  $\frac{11}{2}^-$  level. The mixed  $M1-E2$  character of the former cascade is suggested by the available partial angular distribution information and corroborated by the existence of strong  $J \rightarrow J-2$  quadrupole crossover transitions of 522, 580, 632, 675, 708, and 728 keV. Likewise, the  $J \rightarrow J-2$  quadrupole character of the latter is also suggested by this partial angular distribution information. These characteristics have been confirmed by Yoshikawa *et al.*<sup>12</sup> in their investigation of  $^{121}\text{Cs}$  using the  $^{112}\text{Sn}(^{12}\text{C}, p2n)^{121}\text{Cs}$  reaction.

No other  $\gamma$  ray has been observed in coincidence with either cascade, indicating that they feed either the ground state or a long lived isomer. A  $\frac{9}{2}^+$  isomer ( $T_{1/2}=2$  min) has been observed in atomic-beam measurements on  $^{121}\text{Cs}$ ; the ground-state spin was measured to be  $\frac{3}{2}^+$ .<sup>13</sup> From the systematics of the band structures on the  $\frac{9}{2}^+$  states in this

region, it can be concluded that the  $\Delta J=1$  cascade is built on the  $\frac{9}{2}^+$  state. From its lifetime, this state is estimated to lie  $\Delta \sim 40$  keV excitation energy. The energy of  $\Delta'$  of the  $\frac{11}{2}^-$  level, which evidently is a long lived isomer, cannot be determined from these results.

The assignment of the  $\frac{9}{2}^+$  and  $\frac{11}{2}^-$  cascades to the same nucleus ( $^{121}\text{Cs}$ ) is strongly suggested by the close similarity of their excitation functions. In Fig. 7, the excitation functions of several of the  $\gamma$  rays assigned to  $^{121}\text{Cs}$  are shown. To eliminate the possibility that these cascades belong to the lower  $Z$  nuclei, some of which are very strongly populated in the  $^{110}\text{Cd} + ^{14}\text{N}$  reaction, singles measurements were performed for the  $^{112}\text{Cd} + ^{12}\text{C}$  reaction, which would only populate nuclei with  $Z \leq 54$ . None of the  $\gamma$  rays assigned to  $^{121}\text{Cs}$  were observed in the singles spectrum, whereas the competing cascades (belonging to the  $Z \leq 54$  nuclei) were observed.<sup>14</sup>

$^{119}\text{Cs}$

From reaction calculations<sup>15</sup> and previous experience, it has been known that the  $[\text{HI}, p(x-1)n]$  reaction channel becomes increasingly stronger compared to the  $[\text{HI}, xn]$  channel for the more neutron deficient nuclei. The  $^{106}\text{Cd}[^{16}\text{O}, p2n]^{119}\text{Cs}$  reaction was, therefore, selected for the study of this nucleus. Typical  $\gamma$ - $\gamma$  spectra for  $^{119}\text{Cs}$  are shown in Fig. 8 and the resulting level scheme is

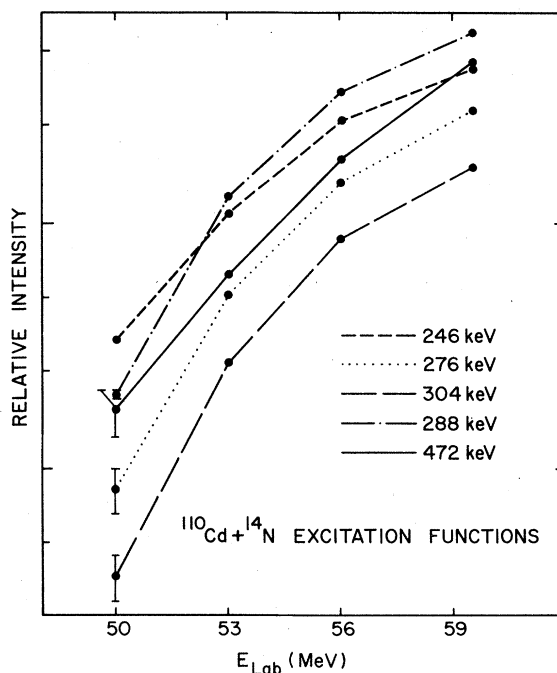


FIG. 7. Excitation functions for several  $\gamma$  rays assigned to  $^{121}\text{Cs}$ .

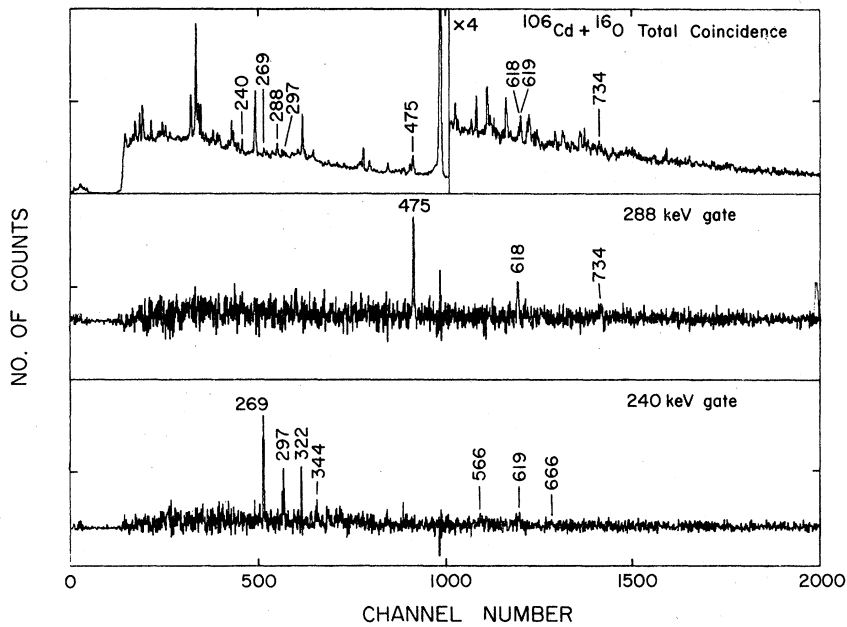


FIG. 8. Typical  $\gamma$ - $\gamma$  spectra for  $^{119}\text{Cs}$ .

presented in Fig. 9.

In  $^{119}\text{Cs}$  also, two distinct cascades have been placed in the level scheme: a  $\Delta J=1$  cascade of 240-, 269-, 297-, 322-, and 344-keV  $\gamma$  rays, and a  $\Delta J=2$  cascade of 288-, 475-, 618-, and 734-keV  $\gamma$  rays. The nature of these transitions is clearly indicated by the available partial angular distribu-

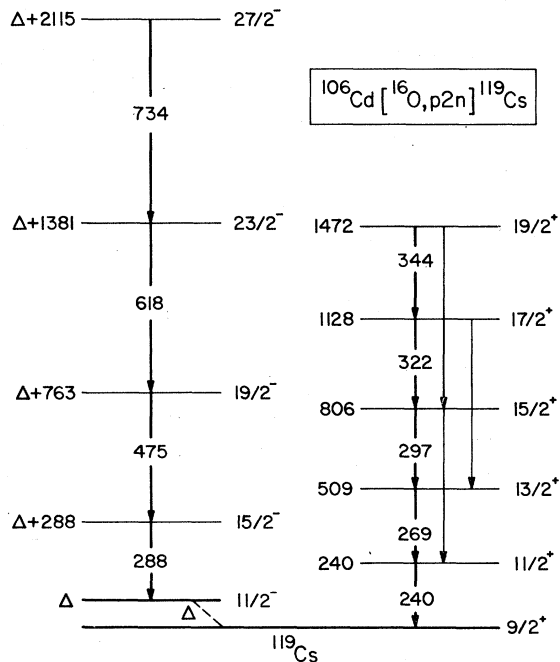


FIG. 9. Level scheme for  $^{119}\text{Cs}$  extracted from the work. All energies are in keV. The energy  $\Delta$  of the  $\frac{11}{2}^-$  level is not known (see text).

tion information and is consistent with the observation of similar band structures in other odd-mass Cs nuclei. The  $M1$ - $E2$  character of the  $\Delta J=1$  cascade is further corroborated by  $J \rightarrow J-2$  quadrupole cross-over transitions of 566, 619, and 667 keV.

No other  $\gamma$  rays have been observed in coincidence with either cascade, suggesting that they feed either the ground state or a long lived isomer. The ground-state spin has been known from atomic-beam measurements to be  $\frac{9}{2}^+$ .<sup>16</sup> Based on the systematics of the bands in this region, the  $\Delta J=1$  cascade is attributed to the  $\frac{9}{2}^+$  ground state and the  $\Delta J=2$  cascade to an  $\frac{11}{2}^-$  state, which evidently is an isomer with a long lifetime. The energy  $\Delta$  of this state cannot be determined from these results. As in the case of  $^{121}\text{Cs}$ , the assignment of these two cascades to the nucleus  $^{119}\text{Cs}$  has been concluded from their excitation functions and the elimination of competing cascades, belonging to the lower- $Z$  nuclei, by means of the  $^{110}\text{Cd} + ^{12}\text{C}$  reaction.<sup>14</sup>

#### IV. DISCUSSION

The two main features observed in the odd-mass Cs isotopes investigated in this work are a series of  $\Delta J=2$  bands built on low-lying  $\frac{11}{2}^-$  states, and a series of  $\Delta J=1$  bands built on low-lying  $\frac{9}{2}^+$  states. The former have been discussed in detail in paper I.<sup>1</sup> The  $\Delta J=1$  bands built on the  $\frac{9}{2}^+$  states in odd-mass Cs nuclei are shown in Fig. 10. The numbers below the bandheads in Fig. 10 represent their excitation energies. The similarity between these  $\Delta J=1$  bands and those previously observed



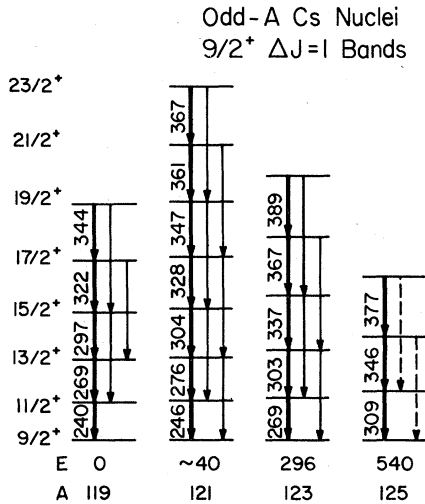


FIG. 10. Systematics of the observed  $\Delta J=1$  bands built on the  $\frac{9}{2}^+$  states in  $^{119-125}\text{Cs}$ . The  $\gamma$ -ray and band-head energies are in keV.

in the odd-mass Sb and I isotopes suggests a collective structure that is common to all of these transitional nuclei. As shown, the band spacings as well as the bandhead energies decrease continuously with  $N$  in going from  $^{125}\text{Cs}$  to  $^{119}\text{Cs}$ ; the bandhead has dropped to become the ground state in  $^{119}\text{Cs}$ .

These  $\Delta J=1$  bands can be interpreted as resulting from the coupling of a  $1g_{9/2}$  quasi-proton hole to a deformed rotor or an anharmonic vibrator. A strongly coupled deformed (prolate) rotor interpretation<sup>17-19</sup> of these  $\frac{9}{2}^+$  bands in odd-mass Cs nuclei is implied by the band spacings, the  $E2-M1$  mixing ratios, the direct-to-crossover intensity ratios and the  $\frac{9}{2}^+$  bandhead energies, as previously shown for the Sb and I  $\frac{9}{2}^+$  bands.<sup>5,20</sup> An anharmonic core plus particle description<sup>21-23</sup> contains several equivalent features and it has been shown by Van Isacker *et al.*<sup>20</sup> that such a description also can describe the  $\frac{9}{2}^+$  bands in these transitional nuclei. A rotational interpretation for these bands is preferred, in our opinion, since the low energies of the  $1g_{9/2}$  proton-hole states are not explained in the anharmonic core model without involving an unreasonably large number of anharmonic phonons.

The energy spacings in these bands are in good agreement with those expected for a rotational model. These band spacings yield moments of inertia  $I$  that are consistent with large deformations. Using the approximate formula for energies of an axially symmetric rigid rotor  $E_J = (\hbar^2/2I)J(J+1)$ , reasonable estimates for  $I$  can be extracted from the energy spacings of the  $\frac{13}{2}^+$  and  $\frac{9}{2}^+$  band members (this choice avoids possible shifts in the  $\frac{11}{2}^+$  band members due to deformation asymme-

tries). The values of  $2I/\hbar^2$  thus extracted for the Cs isotopes are 47.2, 46.0, 42.0, and 36.6  $\text{MeV}^{-1}$  for  $^{119}\text{Cs}$ ,  $^{121}\text{Cs}$ ,  $^{123}\text{Cs}$ , and  $^{125}\text{Cs}$ , respectively. The maximum value, 47.2  $\text{MeV}^{-1}$  for  $^{119}\text{Cs}$ , compares with the maximum values of 39.5 and 34.2  $\text{MeV}^{-1}$  obtained for  $^{119}\text{I}$  and  $^{121}\text{Sb}$ , respectively, showing a continuous increase in  $I$  with an increase in  $Z$ .

Detailed calculations have been performed for a  $1g_{9/2}$  proton hole coupled to a deformed rotor, using the model of Meyer-ter-Vehn.<sup>18,19</sup> Figure 11 shows a comparison of the calculated level energies with the experimental values. The solid circles represent the calculated energies of the band members; the deformation parameter  $\beta$ , and the Fermi energy parameter FER are given, for each isotope, under the bandheads. The parameter FER is defined in such a way that, for a hole spectrum, FER=0 corresponds to the Fermi level situated on the highest single particle state of the  $j$  shell, FER=1 to the second highest single particle state, and other values are interpolated or extrapolated linearly from these points. The pairing potential was chosen as  $\Delta = (135/A)$  MeV. The values of  $\beta$  and FER were varied to obtain the best fits for the  $\frac{11}{2}^+$  and  $\frac{13}{2}^+$  levels. The values of  $\beta$  thus obtained increase smoothly from  $^{125}\text{Cs}$  to  $^{119}\text{Cs}$ , implying increased deformation for the lower-mass Cs isotopes; the positions of the Fermi levels are consistent with Hartree-Fock calculations of occupation probabilities of various orbitals in this region.<sup>24</sup> The inclusion of  $\gamma$  asymmetry did not

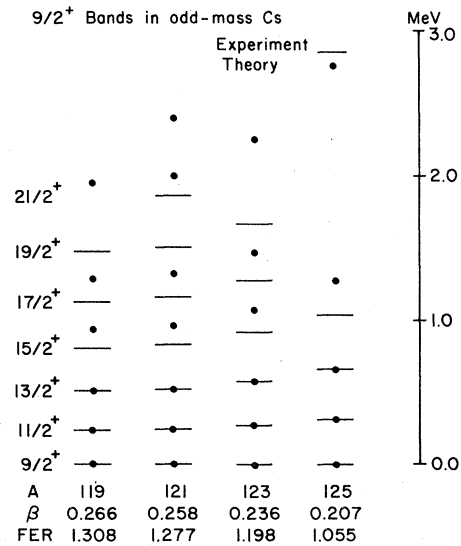


FIG. 11. Comparison of experimental and calculated energy levels for  $\Delta J=1$  bands in  $^{119-125}\text{Cs}$ . The filled circles represent the calculated levels.  $\beta$  and FER are the deformation and Fermi-energy parameter, respectively (see text).

significantly affect the results by the criterion mentioned above, although in some cases a value of  $\gamma \sim 15^\circ$  produced slightly better fits for some of the higher levels.

As shown in Fig. 11, the agreement of the calculated energy levels with the experimental values worsens for the higher  $J$  states. This is expected, since these calculations employ a fixed moment of inertia  $I_0$  for the core and do not take into account the changes in  $I_0$  because of high-spin centrifugal stretching. These deviations can be reduced by the inclusion of core softness, as Toki and Faessler<sup>25</sup> have shown, using a variable moment of inertia  $I$ . The  $\beta$  values, however, are not expected to change significantly from those obtained from the present calculations.

Further evidence for the rotational interpretation of the Cs  $\frac{9}{2}^+$  bands is obtained from the experimental mixing ratios  $\delta(E2/M1)$  of the  $J \rightarrow J-1$  transitions as well as the direct to crossover intensity ratios within the bands. Although, because of their large uncertainties, the experimental mixing ratios do not provide a sensitive measure of the quadrupole moment  $Q_0$ , the angular distributions for each case, nevertheless, clearly show that  $\delta(E2/M1) > 0$  for the band members. Hence,  $Q_0$  must be positive, implying a prolate deformation.<sup>26</sup> The observed ratios of the intensity of the  $J \rightarrow J-1$  transition to the intensity of the  $J \rightarrow J-2$  transition are also consistent with the rotor interpretation.

The  $\frac{9}{2}^+$  bandhead energies, which unexpectedly drop to the ground state in <sup>119</sup>Cs, can be understood on the basis of the Nilsson proton-hole orbitals available at prolate deformations. The  $[404] \frac{9}{2}^+$  orbital rises sharply for prolate deformations; thus the state formed by exciting a proton out of the  $[404] \frac{9}{2}^+$  orbital would decrease in energy with an increase in deformation, provided that the core is soft to deformations. Detailed calculations for the energies of these  $\frac{9}{2}^+$  proton-hole states have been performed by Van Isacker *et al.*<sup>20</sup> for Sb, and Fossan *et al.*<sup>4</sup> for I isotopes; they were found to be in good agreement with the experiments. Similar calculations for Cs isotopes by Heyde *et al.*<sup>27</sup> show minima in energies of these states for  $\beta \sim 0.25$ , which are appropriate as seen in the level-spacing calculations described earlier. These arguments suggest that the  $\frac{9}{2}^+$  bandheads in the odd-mass Cs nuclei are deformed 6p-1h states, similar to the 4p-1h and 2p-1h states in the I and Sb nuclei, respectively, with the proton hole in the  $[404] \frac{9}{2}^+$  orbital.

The excitation energies of the  $\frac{9}{2}^+$  bandheads in odd-mass Cs isotopes are plotted and compared with those for the Sb and I isotopes in Fig. 12. The Cs bandhead energies appear to be following

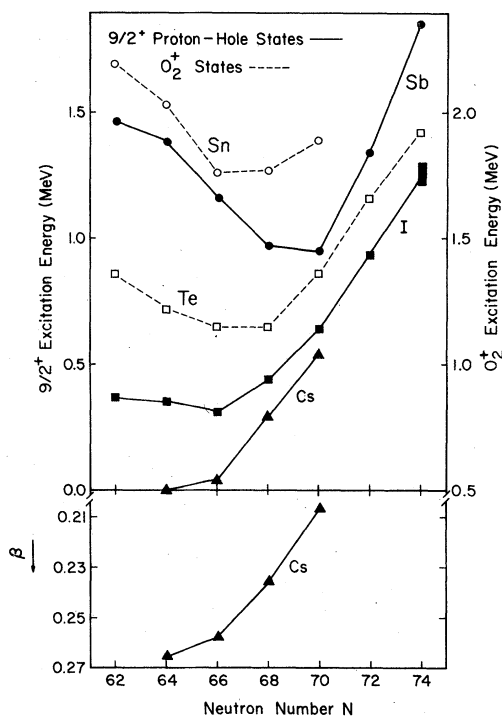


FIG. 12. The  $\frac{9}{2}^+$  bandhead energies for odd-mass Sb, I, and Cs nuclei and  $0_2^+$  energies of even-mass Sn and Te nuclei plotted against the neutron number  $N$ . The lower part shows  $\beta$  for the Cs  $\frac{9}{2}^+$  bands, on an inverted scale (see text).

a parabola-like curve, similar to those for the Sb and I isotopes, with the minimum energy occurring at  $N \approx 64$ . A comparison, as a function of  $N$ , of the  $\frac{9}{2}^+$  bandhead energies and the deformations extracted from the  $\Delta J = 1$  band spacings can show the extent to which the deformation influences these excitation energies. The deformations  $\beta$ , which have been obtained for Cs isotopes from the calculations described earlier, are plotted on an inverted scale as a function of the neutron number  $N$ , in the lower part of Fig. 12. The curves drawn through the  $\frac{9}{2}^+$  bandhead energies and the  $\beta$  values for the Cs isotopes are correlated in shape, implying that the deformation of the core is a dominant factor in the reduction of the  $\frac{9}{2}^+$  excitation energies from the large values ( $\sim 4$  MeV) expected for spherical  $1g_{9/2}$  proton-hole states. Similar comparisons for the Sb and I isotopes have shown slight differences in the shapes of the two curves, suggesting that the detailed neutron-proton and pairing interactions are also causing some variations as a function of  $N$ .

To further extend the  $\frac{9}{2}^+$   $\Delta J = 1$  band systematics as a function of the proton number  $Z$ , a search was initiated for similar band structures in the odd-mass La ( $Z = 57$ ) nuclei. In this search, that

involved a remeasurement with the  $^{112}\text{Sn}(^{16}\text{O}, p2n)^{125}\text{La}$  reaction, a  $\Delta J=1$  band consisting of 211-, 231-, 285-, and 330-keV  $\gamma$  rays, built on the  $\frac{9}{2}^+$  state was observed.<sup>28</sup> For comparison, the systematics of the  $\Delta J=1$  bands built on the  $\frac{9}{2}^+$  states in the  $N=68$  isotones  $^{119}\text{Sb}$ ,  $^{121}\text{I}$ ,  $^{123}\text{Cs}$ , and  $^{125}\text{La}$ , are shown in Fig. 13. As the proton number  $Z$  increases, the band spacings decrease, implying increasing moments of inertia and deformations; the values of  $2I/\hbar^2$ , extracted from these band spacings are 34.0, 37.3, 42.0, and 54.3  $\text{MeV}^{-1}$ , respectively, for  $^{119}\text{Sb}$ ,  $^{121}\text{I}$ ,  $^{123}\text{Cs}$ , and  $^{125}\text{La}$ . In detailed energy level calculations, using the model of Meyer-ter-Vehn, the values of the deformation parameter  $\beta$ , extracted from best fits to the  $\frac{11}{2}^+$  and  $\frac{13}{2}^+$  levels, vary smoothly, increasing with the proton-number  $Z$  (from the equivalent of 0.206 in  $^{119}\text{Sb}$  to 0.267 in  $^{125}\text{La}$ ).

A deformed-structure relationship between the excitation of a  $1g_{9/2}$  proton and the excitation of a pair of  $1g_{9/2}$  protons across the  $Z=50$  closed shell has been established by the observation, via  $(\alpha, 2n)$  reactions, of rotational bands on low-lying deformed  $0_2^+$  states in the even-mass Sn ( $Z=50$ ) nuclei.<sup>7</sup> These 2p-2h states show large  $L=0$  Cd ( $^3\text{He}, n$ ) strengths<sup>29</sup> implying a significant  $(1g_{9/2})^{-2}$  contribution. The moments of inertia  $I$  extracted from these  $A-1$ Sn  $0_2^+$  band spacings are greater than or equal to those extracted from the  $\frac{9}{2}^+$  band spacings in the neighboring  $A$ Sb nuclei. Moreover, the parabola-like curves connecting the Sn  $0_2^+$  and Sb  $\frac{9}{2}^+$  states have similar shapes and minima as a function of  $N$ ; the Sn  $0_2^+$  energies are plotted in the upper part of Fig. 12 for comparison. These features indicate that these  $\Delta J=1$  bands built on the  $\frac{9}{2}^+$  states in odd-mass  $A$ Sb isotopes are perhaps better represented by the coupling of a  $1g_{9/2}$  proton to the deformed 2p-2h  $0_2^+$  states in the corresponding  $A-1$ Sn nuclei, than by the coupling of a  $1g_{9/2}$

proton hole to the 2p ground states of the  $A+1$ Te nuclei.

By the above relationship, the deformed 4p-1h and 6p-1h  $\frac{9}{2}^+$  states in the odd-mass I and Cs isotopes would suggest deformed 4p-2h and 6p-2h  $0^+$  states in the even-mass Te ( $Z=52$ ) and Xe ( $Z=54$ ) nuclei. Preliminary results from the investigation of even-mass Te nuclei at Stony Brook by Chowdhury *et al.*<sup>30</sup> indicate the existence of deformed rotational bands, evidently built on  $0^+$  states in  $^{118,120,122}\text{Te}$ ; the bandhead energies, however, have not yet been determined. Nevertheless, the known  $0_2^+$  states in the even-mass Te isotopes<sup>31</sup> have an energy dependence on  $N$  which is similar to that of the  $\frac{9}{2}^+$  states in the I isotopes. These  $0_2^+$  states, which are also shown in the upper part of Fig. 12, could possibly include significant 4p-2h components;  $0^+$  states of a different structure are also possible at these energies in the Te nuclei. Only preliminary information is available on the excited  $0^+$  states in the even-mass Xe nuclei<sup>32</sup>; no rotational band structures have so far been identified thereon. The complete systematics of the deformed  $\frac{9}{2}^+$  proton-hole states determined out to the Cs isotopes point to the need for a search of low-lying deformed  $0^+$  states in the Xe isotopes.

## V. SUMMARY

This paper, together with paper I,<sup>1</sup> presents results of studies on the collective properties of the odd-mass  $^{119-133}\text{Cs}$  nuclei, using techniques of in-beam  $\gamma$ -ray spectroscopy following heavy-ion fusion-evaporation reactions. Three collective nuclear structure features have been observed:  $\Delta J=1$  bands built on the  $\frac{9}{2}^+$  proton-hole states in  $^{119-125}\text{Cs}$ ,  $\Delta J=2$  bands built on the  $1h_{11/2}$  quasi-proton states in all of these Cs isotopes, and  $\Delta J=2$  bands built on the  $1g_{7/2}$  quasi-proton states in  $^{125-133}\text{Cs}$ .

The  $\frac{9}{2}^+$  bandheads are believed to result from the excitation of a  $1g_{9/2}$  proton across the  $Z=50$  closed shell; these states have been observed in Cs isotopes at surprisingly low energies, becoming the ground state in  $^{119}\text{Cs}$ . The  $\Delta J=2$  bands generally have spacings that are closely related to the spacings in the ground-state bands in the neighboring even-even Xe core nuclei. For the  $\frac{11}{2}^-$  bands in the lowest-mass isotopes, however, there is a significant deviation from the core spacings.

These collective properties can be explained reasonably well in terms of both the particle-plus-rotor and the particle-plus-vibrator models. A comparative study of the systematics of these band structures in the odd-mass Sb, I, Cs, and La nuclei, however, seems to indicate that the

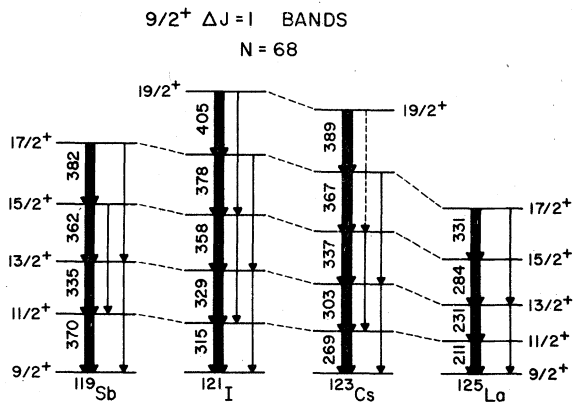


FIG. 13. Systematics of the observed  $\Delta J=1$  bands built on the  $\frac{9}{2}^+$  states in the  $N=68$  isotones,  $^{119}\text{Sb}$ ,  $^{121}\text{I}$ ,  $^{123}\text{Cs}$ , and  $^{125}\text{La}$ . The  $\gamma$ -ray energies are in keV.

vibrational effects become increasingly influential as the proton number approaches the  $Z = 50$  closed shell.

A deformed-structure relationship between the excitation of a  $1g_{9/2}$  proton and the excitation of a pair of  $1g_{9/2}$  protons across the  $Z = 50$  closed shell has been discussed. The  $\frac{9}{2}^+$   $2p-1h$ ,  $4p-1h$ , and  $6p-1h$  states in the odd-mass Sb, I, and Cs nuclei,

respectively, could possibly be understood in terms of the coupling of a  $1g_{9/2}$  proton to deformed  $2p-2h$ ,  $4p-2h$ , and  $6p-2h$   $0^+$  states in the even-even Sn, Te, and Xe nuclei, respectively.

This work was supported in part by the National Science Foundation.

\*Present address: Cyclotron Inst., Texas A & M Univ., College Station, Tx. 77843.

†Present address: Indiana Univ. Cyclotron Facility, Bloomington, In. 47401.

<sup>1</sup>U. Garg, T. P. Sjoreen, and D. B. Fossan, preceding paper, Phys. Rev. C **19**, 207 (1979).

<sup>2</sup>M. Conjeaud, S. Harrar, M. Caballero, and N. Cindro, Nucl. Phys. **A215**, 383 (1973).

<sup>3</sup>R. E. Anderson, P. A. Batay-Csorba, R. A. Emigh, D. A. Lind, P. A. Smith, C. D. Zafiratos, and W. P. Alford, Bull. Am. Phys. Soc. **22**, 1025 (1977).

<sup>4</sup>D. B. Fossan, M. Gai, A. K. Gaigalas, D. M. Gordon, R. E. Shroy, K. Heyde, M. Waroquier, H. Vincx, and P. Van Isacker, Phys. Rev. C **15**, 1732 (1977).

<sup>5</sup>K. Heyde, M. Waroquier, H. Vincx, and P. Van Isacker, Phys. Lett. **64B**, 135 (1976).

<sup>6</sup>U. Garg, T. P. Sjoreen, and D. B. Fossan, Phys. Rev. Lett. **40**, 831 (1978).

<sup>7</sup>J. Bron, W. H. A. Hesselink, L. K. Peker, A. Van Poelgeest, J. Uitzinger, H. Verheul, and J. Zalmstra, J. Phys. Soc. Jpn. **44**, Suppl. 513 (1978).

<sup>8</sup>U. Garg, T. P. Sjoreen, and D. B. Fossan, Bull. Am. Phys. Soc. **21**, 1003 (1976); and **22**, 595 (1025) (1977); and in *Proceedings of the International Conference on Nuclear Structure, Tokyo, 1977*, edited by T. Marumori (International Academic Printing Co., Tokyo, 1977), p. 360.

<sup>9</sup>R. Arlt, A. Jasinski, W. Neubert, and H. G. Ortlepp, Acta. Phys. Pol. **B6**, 433 (1976).

<sup>10</sup>E. Der Mateosian and A. W. Sunyar, At. Data and Nucl. Data Tables **13**, 391, 407 (1974).

<sup>11</sup>G. Beyer, R. Arlt, E. Hermann, A. Jasinski, O. Knotek, G. Musiol, H. G. Ortlepp, H. V. Siebert, and J. Tyrroff, Nucl. Phys. **A260**, 269 (1976).

<sup>12</sup>N. Yoshikawa, J. Gizon, and A. Gizon, J. Phys. (Paris) Lett. **39**, L-102 (1978).

<sup>13</sup>C. Ekstrom, S. Ingelman, G. Wannberg, and M. Skare-

stad, Nucl. Phys. **A202**, 144 (1977).

<sup>14</sup>U. Garg, P. Chowdhury, T. P. Sjoreen, and D. B. Fossan (unpublished).

<sup>15</sup>Code ALICE, M. Blann, USAEC Report No. OOO-3494-029 (unpublished).

<sup>16</sup>H. Fischer, P. Dabkiewicz, P. Freiling, H. J. Klunge, H. Kremmling, R. Neugart, and E. W. Otten, Z. Phys. **A284**, 3 (1978).

<sup>17</sup>F. S. Stephens, Rev. Mod. Phys. **47**, 43 (1975).

<sup>18</sup>J. Meyer-ter-Vehn, F. Stephens, and R. M. Diamond, Phys. Rev. Lett. **32**, 1383 (1974).

<sup>19</sup>J. Meyer-ter-Vehn, Nucl. Phys. **A249**, 111, 141 (1975).

<sup>20</sup>P. Van Isacker, M. Waroquier, H. Vincx, and K. Heyde, Nucl. Phys. **A292**, 125 (1977).

<sup>21</sup>U. Hageman and F. Donau, Phys. Lett. **59B**, 121 (1975).

<sup>22</sup>G. Alaga and V. Paar, Phys. Lett. **61B**, 219 (1976).

<sup>23</sup>A. Arima and F. Iachello, Phys. Rev. C **14**, 761 (1976).

<sup>24</sup>D. Strottman, private communication.

<sup>25</sup>H. Toki and A. Faessler, Nucl. Phys. **A253**, 231 (1975).

<sup>26</sup>K. Nakai, Phys. Lett. **34B**, 269 (1971).

<sup>27</sup>K. Heyde *et al.*, private communication.

<sup>28</sup>U. Garg, P. Chowdhury, T. P. Sjoreen, and D. B. Fossan, Bull. Am. Phys. Soc. **23**, 90 (1978).

<sup>29</sup>H. W. Fielding, R. E. Anderson, C. D. Zafiratos, D. A. Lind, F. E. Cecil, W. H. Wieman, and W. P. Alford, Nucl. Phys. **A281**, 389 (1977).

<sup>30</sup>P. Chowdhury, W. F. Piel, Jr., U. Garg, and D. B. Fossan, Bull. Am. Phys. Soc. **23**, 962 (1978).

<sup>31</sup>Nuclear Level Schemes  $A = 45$  through  $A = 257$  from Nucl. Data Sheets, edited by Nuclear Data group (Academic, New York, 1973); H. W. Fielding, R. E. Anderson, P. D. Kunz, D. A. Lind, C. D. Zafiratos, and W. P. Alford (unpublished).

<sup>32</sup>R. A. Emigh, R. E. Anderson, P. A. Batay-Csorba, D. A. Lind, P. A. Smith, C. D. Zafiratos, and W. P. Alford, Bull. Am. Phys. Soc. **22**, 1007 (1977).